

RESEARCH ARTICLE OPEN ACCESS

Design and Synthesis of Novel Purine Analogues as Potential IL-1 β Inhibitors Targeting Vascular Inflammation

Dimitra T. Pournara¹ | Theano Fotopoulou¹ | Geena Paramel² | Madelene Lindkvist² | Magnus Grenegård² | Karin Fransén² | Maria Koufaki¹ 

¹Institute of Chemical Biology, National Hellenic Research Foundation, Athens, Greece | ²Faculty of Medicine and Health, Cardiovascular Research Centre, Örebro University, Örebro, Sweden

Correspondence: Maria Koufaki (mkoufa@eie.gr)

Received: 4 August 2025 | **Revised:** 9 November 2025 | **Accepted:** 29 November 2025

Keywords: human aortic smooth muscle cells | IL-1 β inhibitors | 6-piperazinyl purines | purines

ABSTRACT

Proinflammatory cytokine interleukin (IL)-1 β is a key mediator of the inflammatory response in atherosclerosis. Targeting IL-1 β represents a new approach for the anti-inflammatory therapy of cardiovascular diseases. Based on our previous data demonstrating that cardioprotective 6-piperazinyl purines can effectively inhibit IL-1 β release in vascular cells, in this study, we present the synthesis of a next generation of purine analogues bearing either a furoxan moiety as a nitric oxide (NO) donor, or a (methylsulfonyl)thio group, a benzothioamide, or a 5-phenyl-3H-1,2-dithiole-3-thione as putative hydrogen sulfide (H₂S) donor moieties. NO and H₂S are gaseous signaling molecules that can reduce vascular inflammation. The new purine analogues were evaluated for their anti-inflammatory activity by assessing their inhibitory effect on the secretion of lipopolysaccharide (LPS)-induced IL-1 β in human aortic smooth muscle cells (HAoSMCs). Our initial findings revealed that compounds bearing a [methylsulfonyl]thio]propanoyl or [methylsulfonyl]thio]hexanoyl group (compounds **MK175** and **MK169**, respectively) could effectively inhibit LPS-induced IL-1 β release in HAoSMCs.

1 | Introduction

Inflammation is an important factor in promoting atherosclerosis, which is one of the underlying factors for cardiovascular diseases (CVDs) [1]. Atherosclerosis and its acute clinical manifestations, like myocardial infarction and ischemic stroke, are the most common CVDs and the main cause of morbidity and mortality worldwide. Accumulation of low-density lipoproteins and chronic inflammation are hallmarks in the pathogenesis of atherosclerosis. Proinflammatory cytokines such as interleukin (IL)-1 β , a driving force for chronic inflammation in atherosclerosis, are synthesized by leukocytes, e.g., activated macrophages. However, in the atherosclerotic lesion, IL-1 β can be produced by

endothelial and vascular smooth muscle cells [2]. The clinical trial CANTOS (Canakinumab Anti-inflammatory Thrombosis Outcome Study) has also shown that reducing inflammation in the absence of concomitant lipid-lowering reduces the rate of cardiovascular events [3]. Although these findings pave the way to new strategies against vascular inflammation, the high cost of an antibody reduces the availability of this possible treatment option for broad populations.

The NOD-like receptor protein 3 (NLRP3) inflammasome, a multi-protein complex that triggers the activation of caspases leading to IL-1 β synthesis and release, has been linked to the pathophysiology of CVD, attracting a tremendous research

Dimitra T. Pournara Affiliation at the time the study was conducted.

This is an open access article under the terms of the [Creative Commons Attribution-NonCommercial-NoDeriv](https://creativecommons.org/licenses/by-nc-nd/4.0/) License, which permits use and distribution in any medium, provided the original work is properly cited, the use is non-commercial and no modifications or adaptations are made.

© 2026 The Author(s). *Chemistry & Biodiversity* published by Wiley-VHCA AG.

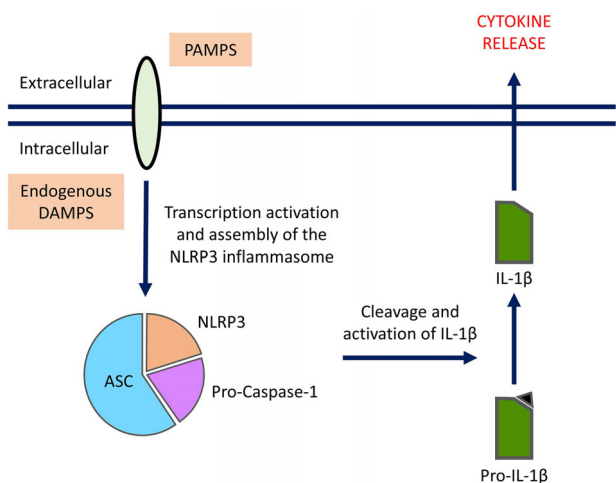


FIGURE 1 | Simplified illustration of NOD-like receptor protein 3 (NLRP3) inflammasome activation, interleukin (IL)-1 β production, and release. Different pathogen-associated molecular patterns (PAMPs), or damage-associated molecular patterns (DAMPs), initiate transcription and assembly of the NLRP3 inflammasome complex, followed by cleavage of pro-IL-1 β into mature IL-1 β , which is released from the cell.

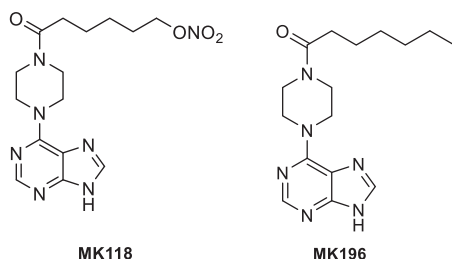


FIGURE 2 | Chemical structures of **MK118** and **MK196**.

interest [4–6]. Experimental data revealed that nitric oxide (NO) [7] can exert anti-inflammatory activity by negatively regulating the activation of the NLRP3 inflammasome [8] (Figure 1). Small molecules bearing organic nitrate esters or the furoxan ring (1,2,5-oxadiazole-2-oxide) have been reported in the literature as putative NO donor groups endowed with various biological activities [9].

The first-generation purine analogue **MK118**, bearing a nitrate ester, and its methyl-substituted analogue **MK196** (Figure 2), both designed and synthesized by our group, were found to reduce the secretion of lipopolysaccharide (LPS)-induced IL-1 β in human aortic smooth muscle cells (HAoSMCs). The study also concluded that the anti-inflammatory effect is independent of NO release by **MK118**, suggesting that these analogues likely influence the NLRP3 inflammasome upstream regulators, thereby imparting an anti-inflammatory effect on HAoSMCs [10].

Besides NO, the gaseous signaling molecule hydrogen sulfide (H₂S) has been increasingly recognized in physiological vessel homeostasis. H₂S is biosynthesized endogenously and is important for the regulation of homeostasis in the cardiovascular system as well as the physiological myocardial function. In addition, several studies demonstrated the therapeutic applications of H₂S, including protection against myocardial ischemia injury, dilation of blood vessels, and regulation of inflammation [11, 12].

It has also been proven that H₂S can reduce the progression of atherosclerotic lesions and vascular inflammation by inhibiting vascular remodeling and abolishing endothelin-induced proliferation of vascular smooth muscle cells [13, 14]. Currently, several research studies are focusing on exploring specific roles of this important gaseous signaling molecule in the attenuation of the NLRP3 inflammasome assembly using both in vitro and in vivo mouse inflammation [15].

In this study, as a continuation of our previous work, we aimed to design and synthesize a next generation of 6-piperazinyl-substituted purine analogues with a NO donor furoxan moiety as well as H₂S donor moieties. We hypothesized that new 6-piperazinyl-substituted purine analogues may exert beneficial anti-inflammatory activity in HAoSMCs.

2 | Results and Discussion

2.1 | Chemistry

The main purine scaffold (**A**) –used for the synthesis of the piperazinyl derivatives – was obtained by protecting the commercially available 6-chloropurine with a tetrahydropyranyl (THP) group using *p*-toluenesulfonic acid monohydrate and 3,4-dihydropyran, followed by heating with piperazine in methanol [16] (**Scheme 1**).

For the synthesis of the potential NO-releasing furoxan derivative **MK170**, bromide **1**, which was prepared as described in our previous publication [17], was attached to piperazine via an alkylation reaction to afford compound **2**. The target compound **MK170** was then obtained by removal of the THP group using either trifluoroacetic acid (TFA) in CH₂Cl₂ or pyridinium *p*-toluenesulfonate (PPTS) in absolute ethanol (EtOH). Methanesulfonothioate [18] and 4-hydroxybenzothioamide, along with 5-(4-hydroxyphenyl)-3H-1,2-dithiole-3-thione (ADT-OH) with reported H₂S releasing properties [19], were used as substituents attached to the new 6-piperazinyl-purine analogues. Sodium methanesulfonothioate and 4-hydroxybenzothioamide, both commercially available, were used as potential H₂S donors along with ADT-OH [20]. In order to investigate the effect of replacing the nitrate ester or methyl group of the previously studied **MK118** and **MK196** purine derivatives by a methanesulfonothioate group on the anti-inflammatory activity, two new piperazinyl purines with different spacer lengths, **MK175** and **MK169**, were synthesized. The three-carbon chain analogue **MK175** was synthesized using 3-bromopropionic acid as a starting material. When heated with sodium methanesulfonothioate in *N,N*-dimethylformamide (DMF) overnight, carboxylic acid **3** was obtained and used for the acylation of purine **A** to afford compound **4**, which was subsequently deprotected with TFA to give purine **MK175**. The purine analogue **MK169** was synthesized based on the structure of compound **MK118**. Heating of bromide **5** with sodium methanesulfonothioate in DMF gave compound **6**. Subsequent deprotection of the THP group with PPTS in absolute EtOH under reflux resulted in compound **MK169**.

Compounds **MK178** and **MK179**, bearing a two-carbon atom spacer linking piperazine and the H₂S donor moiety, were prepared by alkylation of purine **A** with bromides **7** and **9**, respectively. Specifically, for **MK178**, two equivalents of

TABLE 1 | Absorption, distribution, metabolism, excretion (ADME) properties of the synthesized purine analogues.

	#rotor	MW	donorHB	acctpHB	QPlogPo/w	QPlogS	QPlog HERG	PSA	clogP
Range	0–15	130–725	0–6	2–20	–2–6.5	–6.5–0.5	> –5	7–200	< 5
MK169	7	412.524	1	11	1.118	–3.583	–4.359	110.859	0.464
MK170	2	378.393	1	8.5	1.395	–3.243	–6.599	109.894	1.578
MK175	4	370.444	1	11	–0.16	–2.274	–3.686	119.997	0.248
MK178	5	383.47	3	8.75	1.914	–3.977	–6.976	98.87	2.163
MK179	4	456.598	1	8.75	3.713	–5.61	–7.317	76.101	4.163

1,2-dibromoethane reacted with 4-hydroxybenzothioamide in the presence of K_2CO_3 to afford bromide **7**. Alkylation of purine **A** was achieved in the presence of triethylamine (TEA) in anhydrous CH_2Cl_2 to give compound **8**, which, upon deprotection with TFA in CH_2Cl_2 , afforded analogue **MK178**. For the synthesis of **MK179**, we used the isolated ADT-OH, whose synthesis was described in our previous publication [20]. Specifically, ADT-OH reacted with 1,2-dibromoethane through a Williamson ether synthesis reaction in the presence of K_2CO_3 to afford bromide **9**. Alkylation of **A** followed to give compound **10**. The final purine analogue **MK179** was obtained after deprotection with TFA in CH_2Cl_2 .

2.2 | Absorption, Distribution, Metabolism, Excretion Properties

The ADME (absorption, distribution, metabolism, excretion) properties of the synthesized purines were also predicted using QikProp (Maestro 9.8) (Table 1). The values of the following selected properties are between the accepted range and allow their biological testing.

2.3 | Biology

The in vitro examination of the novel synthesized purine analogues would allow the identification of the required structural features for optimum activity. The potency of the tested compounds could additionally help shed light on their mechanism of action and their role in the NLRP3 signaling pathway.

2.3.1 | Effect on IL-1 β Release

This study includes an initial screening of new compounds, aimed at distinguishing active from inactive ones in a relevant inflammatory model in vitro. Our results showed that LPS induced a significant increase in IL-1 β release from HAoSMCs (Figure 3). The purine analogues were evaluated for their role in IL-1 β release using HAoSMCs (Figure 4). Our in vitro results revealed that **MK175**, where piperazine and the methane-sulfonothioate group are linked through an amide bond with a two-carbon chain, effectively reduced the LPS-induced IL-1 β release (Figure 4B). **MK169**, bearing a five-carbon chain, almost completely abolished the IL-1 β secretion from HAoSMCs (Figure 4C). The direct attachment of a putative NO donor group to the piperazine, i.e., the furoxan ring in **MK170**, induced a non-significant trend of

increased IL-1 β release, both by **MK170** alone and in combination with LPS treatment (Figure 4A). Furthermore, the other two purine analogues bearing putative H₂S donor groups, **MK178** and **MK179**, did not inhibit basal or LPS-induced IL-1 β secretion from HAoSMCs (Figure 4D,E).

The initial screening of the novel 6-piperazinyl-substituted purine analogues in the selected biological assay (i.e., HAoSMCs and IL-1 β production) revealed that the furoxan ring bearing **MK170** tends to increase LPS-induced IL-1 β release. The mechanism underlying this potential and unexpected pro-inflammatory activity is presently unknown. Possible explanation may involve the generation of peroxyxynitrite or other so far unknown drug mechanism. Moreover, it seems that attaching putative H₂S donors to the 6-piperazinyl-purines via a short ethylene spacer, as in **MK178** and **MK179**, does not cause anti-inflammatory activity, whereas replacement of the nitrate ester or methyl group of the previously investigated compounds **MK118** (Figure 4F) and **MK196** [10] by a (methylsulfonyl)thio group to create **MK175** and **MK169**, resulted in significant anti-inflammatory activity. In addition, based on the results, we suggest that the spacer length in the active compounds **MK175** and **MK169** does not play an important role, while the attachment to the piperazine ring through an amide bond appears to influence the activity of the synthesized compounds.

3 | Conclusions

Although a precise comparison between the synthesized purines is not possible, it seems that attaching putative H₂S donor groups to the 6-piperazinyl-purines via a short ethylene spacer (**MK178** and **MK179**) does not induce anti-inflammatory activity, whereas replacement of the nitrate ester or methyl group of the previously investigated compounds **MK118** and **MK196** by a (methylsulfonyl)thio group (**MK175** and **MK169**) resulted in significant anti-inflammatory activity. Further investigation of the active compounds will provide concentration curves and will clarify molecular mechanisms of action and the exact identification of the structural features that affect the IL-1 β secretion levels.

4 | Experimental

4.1 | Chemistry

Commercial reagents and solvents were obtained from Acros Organics, Fluka, Merck, Sigma-Aldrich, or Fluorochem in the qualities puriss., p.a., or purum and used without further

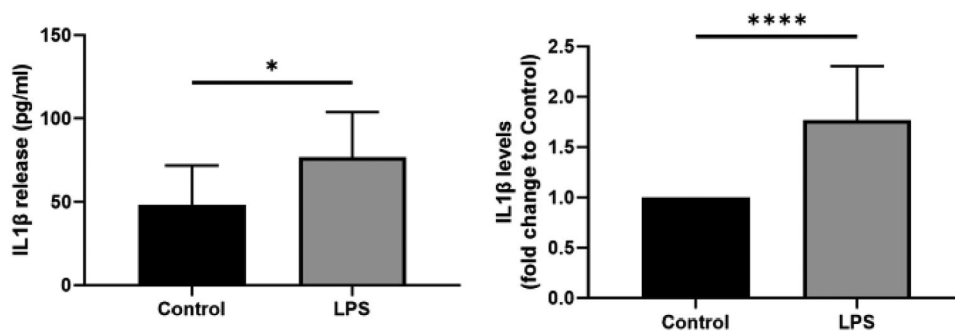


FIGURE 3 | Effect of lipopolysaccharide (LPS) on IL-1 β secretion from human aortic smooth muscle cells (HAoSMCs). Levels of IL-1 β in cell culture media were analyzed after 24 h exposure of HAoSMCs to 100 ng/mL of LPS. Absolute values (left) and normalized control (right). Data are shown as mean values \pm SD ($n = 3$). Statistical differences were analyzed using an unpaired t-test, * $p < 0.05$ and **** $p < 0.0001$.

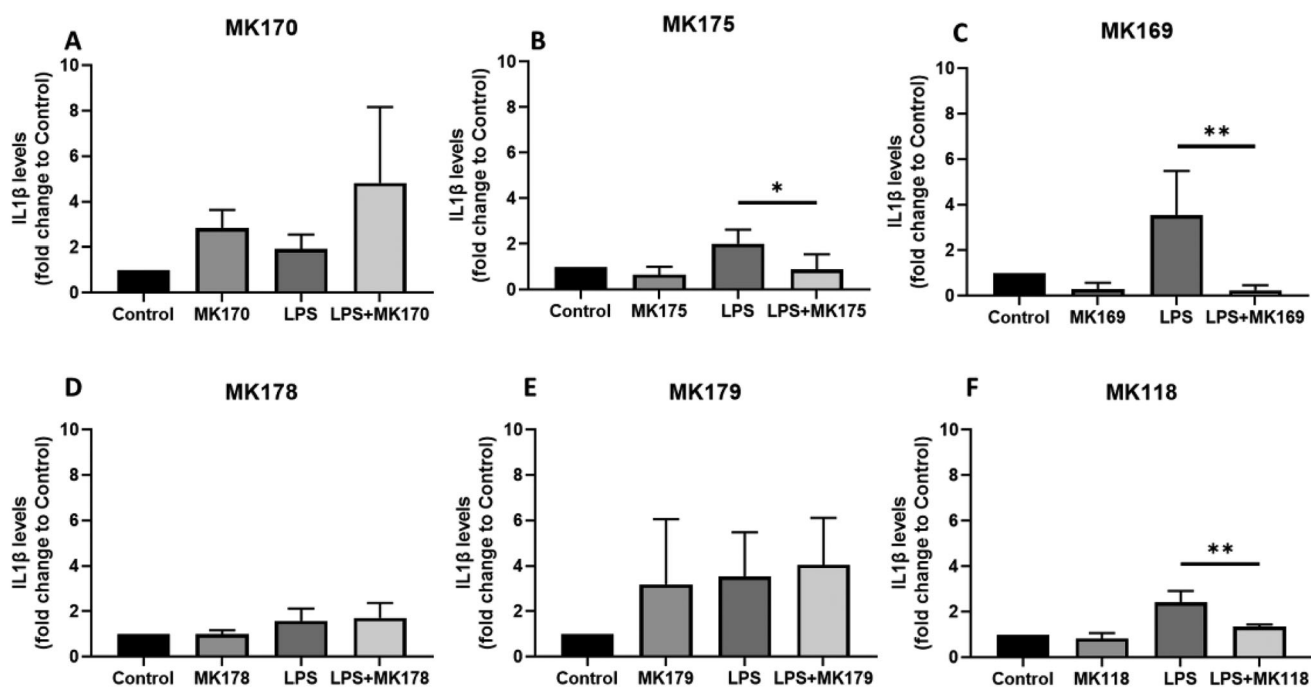


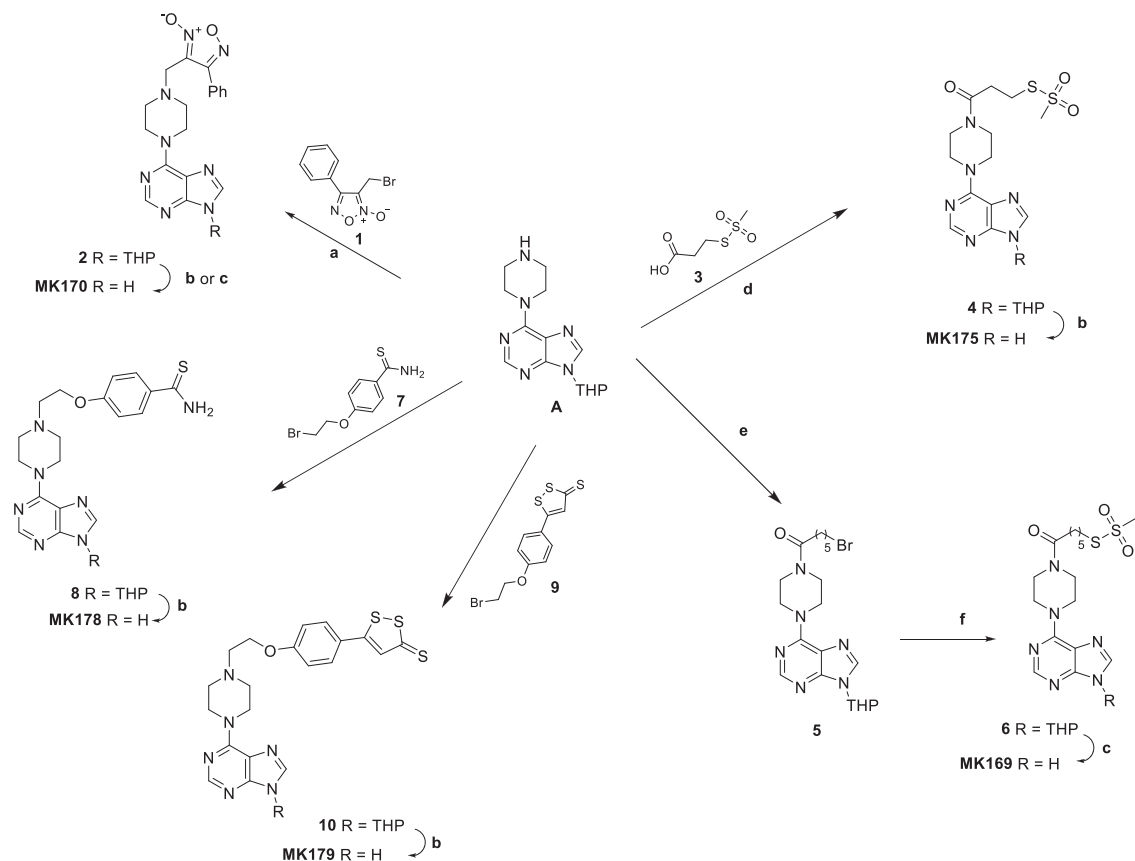
FIGURE 4 | Effect of novel 6-piperazinyl-substituted purine analogues on interleukin (IL)-1 β secretion from human aortic smooth muscle cells (HAoSMCs). Levels of IL-1 β in cell culture media were analyzed after 24 h exposure of HAoSMCs to 30 μ g/mL of various purine analogues (MK170, MK175, MK169, MK178, MK179, and MK118) as indicated in the bar graphs. The activity of the purine analogues was analyzed on basal (bars to the left in each panel, respectively) and LPS (100 ng/mL)-stimulated (bars to the right in each panel, respectively) IL-1 β release. Data are shown as mean values \pm SD ($n = 3$). Statistical differences were analyzed by One-way analysis of variance (ANOVA). * $p < 0.05$ and ** $p < 0.01$.

purification. All non-aqueous reactions were set up under an argon atmosphere, utilizing glassware that was flame-dried and cooled under vacuum. Thin-layer chromatography (TLC) was performed using precoated SiO₂ aluminum plates (Macherey-Nagel Sil G-25 UV254). Chromatographic purification was performed with silica gel (200–400 mesh). ¹H and ¹³C nuclear magnetic resonance (NMR) spectra were recorded on Varian spectrometers operating at 300 or 600 MHz/75 or 150 MHz, respectively, at 25°C using CDCl₃, DMSO-*d*₆, CD₃OD, and acetone-*d*₆. Processing and evaluation of spectra were performed using the program MestReNova 9.0 (Mestrelab Research SL, Santiago de Compostela, Spain). The resonance multiplicity is indicated as s (singlet), d (doublet), t (triplet), and m (multiplet) or combinations of them. Coupling constants (*J*) are given in Hz. Mass spectra were obtained on high-performance

liquid chromatography-mass spectrometry (HPLC–MS)ⁿ Fleet-Thermo, in the electrospray ionization (ESI) mode. High-resolution MS (HRMS) spectra were recorded in the ESI mode, on ultra-performance LC (UPLC)–MSⁿ Orbitrap Velos-Thermo. The microwave-assisted experiments were carried out with a CEM Discover 300 W monomode microwave instrument.

4.1.1 | 6-[4-[(3-Methyl-4-phenyl)-1,2,5-oxadiazole-2-oxide]-piperazin-1-yl]-9-(tetrahydropyran-2-yl)-9H-purine (2)

Piperazinyl purine A (0.25 g, 0.87 mmol) was dissolved in 10 mL anhydrous CH₂Cl₂. Bromide 1 (0.22 g, 0.87 mmol) [17] was added, followed by TEA (0.5 mL, 3.6 mmol). After stirring at room



SCHEME 1 | Reagents and conditions: (a) triethylamine (TEA), CH_2Cl_2 , rt, 20–24 h; (b) trifluoroacetic acid (TFA), CH_2Cl_2 , rt, 30 min; (c) pyridinium *p*-toluenesulfonate (PPTS), EtOH, rt, 18 h; (d) EDC.HCl, TEA, CH_2Cl_2 , rt, 3 h; (e) bromohexanoic acid, CDI, THF, rt; (f) methanesulfonylthioate sodium salt, *N,N*-dimethylformamide (DMF), 65–70°C.

temperature for 20 h, H_2O was added, and the organic layer was extracted with CH_2Cl_2 . The collected organic layers were washed with saturated aqueous NaCl solution and dried over Na_2SO_4 . Column chromatography (Pet. Ether/EtOAc 2:8 v/v) of the filtered crude residue afforded **2** as a yellowish solid (0.13 g, 33% yield). $R_f = 0.45$ (Pet. Ether/EtOAc 2:8 v/v); ^1H NMR (300 MHz, CDCl_3): δ 8.32 (s, 1H, H-2, purine), 7.97–7.94 (m, 2H, ArH), 7.92 (s, 1H, H-8, purine), 7.53–7.50 (m, 3H, ArH), 5.69 (dd, $J = 10.2$ and 2.3 Hz, 1H), 4.28 (bs, 4H, CH_2 -piperazine), 4.13 (d, $J = 9.9$ Hz, 1H), 3.74 (t, $J = 11.4$ Hz, 1H), 3.56 (s, 2H, CH_2N), 2.65–2.62 (m, 4H, CH_2 -piperazine), 2.07–1.58 (m, 6H); ^{13}C NMR (75 MHz, CDCl_3): δ 157.6, 153.8, 152.4, 150.3, 136.3, 131.2, 129.2, 128.1, 126.9, 119.9, 112.5, 81.7, 68.9, 53.0, 52.6, 50.2, 33.8, 25.0, 22.9; ESI-HRMS (m/z): calcd. for $\text{C}_{23}\text{H}_{27}\text{N}_8\text{O}_3$ [$\text{M}+\text{H}$] $^+$ 463.2201; found 463.2197.

4.1.2 | 6-[4-[(3-Methyl-4-phenyl)-1,2,5-oxadiazole-2-oxide]-piperazin-1-yl]-9H-purine (MK170)

The THP-protected purine **2** (0.13 g, 0.28 mmol) was dissolved in 3 mL anhydrous CH_2Cl_2 , and TFA (1.08 mL, 14.2 mmol) was added dropwise. The reaction mixture was stirred at room temperature for 30 min, diluted with 3 mL CH_2Cl_2 , and quenched with saturated aqueous NaHCO_3 solution to reach pH 9–10. Na_2SO_4 was added, and the mixture was stirred for 20 min. After filtration through celite, the filtrate was purified by flash column chromatography (CH_2Cl_2 : CH_3OH 98:2 to 95:5 v/v) to

afford **MK170** as a white solid (0.065 g, 61% yield); $R_f = 0.25$ (CH_2Cl_2 : CH_3OH 95:5 v/v); melting point (m.p.): 234.0–235.0°C; ^1H NMR (300 MHz, $\text{DMSO}-d_6$): δ 13.03 (bs, 1H, NH), 8.19 (s, 1H, H-2), 8.10 (s, 1H, H-8), 8.01–7.97 (m, 2H, ArH), 7.62–7.60 (m, 3H, ArH), 4.17 (bs, 4H, CH_2 -piperazine), 3.62 (s, 2H, CH_2N), 2.54 (t, $J = 5.0$ Hz, 4H, CH_2 -piperazine); ^{13}C NMR (75 MHz, $\text{DMSO}-d_6$): δ 157.7, 153.0, 151.8, 151.5, 138.3, 131.2, 129.2, 128.0, 126.5, 118.8, 113.0, 52.3, 49.7, 44.4; ESI-HRMS (m/z): calcd. for $\text{C}_{18}\text{H}_{19}\text{N}_8\text{O}_2$ [$\text{M}+\text{H}$] $^+$ 379.1625; found: 379.1621.

4.1.3 | 6-[4-[3-(Methylsulfonyl)thio]propanoyl]-piperazin-1-yl]-9-(tetrahydropyran-2-yl)-9H-purine (4)

To a solution of **A** (0.05 g, 0.16 mmol) in anhydrous CH_2Cl_2 (3 mL), 3-((methylsulfonyl)thio)propanoic acid (**3**) (0.06 g, 0.33 mmol), EDC hydrochloride (0.09 g, 0.49 mmol), and TEA (0.13 mL, 0.98 mmol) were added. The resulting mixture was stirred at room temperature for 3 h. H_2O was added, and the aqueous phase was extracted with CH_2Cl_2 . The combined organic layers were dried over Na_2SO_4 , filtered, and concentrated in vacuo. Flash column chromatography (CH_2Cl_2 / CH_3OH , 98:2 v/v) afforded **4** as a colorless oil in 65% yield (0.05 g). $R_f = 0.36$ (CH_2Cl_2 / CH_3OH 95:5 v/v); ^1H NMR (300 MHz, CDCl_3): δ 8.37 (s, 1H, H-2), 7.97 (s, 1H, H-8), 5.73 (dd, $J = 10.3$ and 2.4 Hz, 1H, CH-THP), 4.35–4.31 (m, 4H, CH_2 -piperazine), 4.16–3.73 (m, 4H), 3.60–3.57 (m, 2H, CH_2 -piperazine), 3.44 (t, $J = 6.4$ Hz, 2H), 3.34 (s,

3H, S₂O₂CH₃), 2.94 (t, *J* = 6.4 Hz, 2H), 2.11–1.65 (m, 6H); ¹³C NMR (75 MHz, CDCl₃): δ 168.9, 153.8, 152.5, 150.5, 136.6, 120.1, 81.8, 69.0, 50.1, 45.4, 42.0, 34.1, 32.0, 31.7, 25.0, 23.0; ESI-HRMS (*m/z*): calcd. for C₁₈H₂₇N₆O₄S₂ [M+H]⁺ 455.1531; found: 455.1535.

4.1.4 | 6-[4-[3-(Methylsulfonyl)thio]propanoyl]-piperazin-1-yl]-9H-purine (MK175)

A solution of **4** (0.02 g, 0.04 mmol) and TFA (0.17 mL, 2.2 mmol) in 2 mL anhydrous CH₂Cl₂ was stirred at room temperature for 25 min. The mixture was diluted with CH₂Cl₂ and quenched with saturated aqueous NaHCO₃ solution till pH 10 was reached. Na₂SO₄ was added, and the suspension was stirred for 20 min and then filtered. The concentrated residue was purified by flash column chromatography (CH₂Cl₂/CH₃OH, 98:2 to 95:5) to afford **MK175** as a white solid (0.009 g, 57% yield); m.p. 203–205°C; *R_f* = 0.16 (CH₂Cl₂/CH₃OH 95:5 v/v); ¹H NMR (300 MHz, DMSO-*d*₆): δ 13.03 (s, 1H, NH), 8.19 (s, 1H, H-2), 8.10 (s, 1H, H-8), 4.22–4.15 (m, 4H, CH₂-piperazine), 3.57–3.51 (m, 4H, CH₂-piperazine), 3.46 (s, 3H, S₂O₂CH₃), 3.30 (t, *J* = 6.4 Hz, 2H), 2.90 (t, 2H, *J* = 6.4 Hz); ¹³C NMR (75 MHz, DMSO-*d*₆): δ 169.0, 153.1, 151.8, 151.5, 138.5, 118.9, 50.0, 44.6, 41.2, 33.2, 31.4; ESI-HRMS (*m/z*): calcd. for C₁₃H₁₉N₆O₃S₂ [M+H]⁺ 371.0956; found: 371.0954.

4.1.5 | 6-[4-[6-(Methylsulfonyl)thio]hexanoyl]-piperazin-1-yl]-9-(tetrahydropyran-2-yl)-9H-purine (6)

Bromide **5** [16] (0.04 g, 0.09 mmol) was dissolved in 1 mL of anhydrous DMF, and methanesulfonylthioate sodium salt (0.02 g, 0.14 mmol) was added. After heating at 65–70°C for 3 h, the mixture was washed with H₂O and saturated aqueous NaCl solution. The aqueous layers were then extracted with EtOAc, and the combined organic layers were dried over Na₂SO₄, filtered, and concentrated in vacuo. The concentrated residue was used in the next step without further purification (0.04 g); *R_f* = 0.34 (CH₂Cl₂/CH₃OH 95:5 v/v); ¹H NMR (600 MHz, CDCl₃): δ 8.34 (s, 1H, H-2), 7.95 (s, 1H, H-8), 5.71–5.69 (m, 1H, CH-THP), 4.38–4.34 (m, 4H, CH₂-piperazine), 4.13 (d, *J* = 11.6 Hz, 1H, CH₂-THP), 3.77–3.72 (m, 3H), 3.59–3.57 (m, 2H, CH₂-piperazine), 3.29 (s, 3H, S₂O₂CH₃), 3.15 (t, *J* = 7.2 Hz, 2H), 2.37 (t, *J* = 7.4 Hz, 2H), 2.08–1.95 (m, 2H), 1.82–1.61 (m, 6H), 1.50–1.45 (m, 2H); ¹³C NMR (75 MHz, CDCl₃): δ 172.0, 153.8, 152.5, 150.2, 136.0, 119.8, 81.7, 68.8, 58.5, 53.4, 50.7, 36.4, 31.9, 29.5, 28.5, 26.9, 26.6, 25.0, 22.9.

4.1.6 | 6-[4-[6-(Methylsulfonyl)thio]hexanoyl]-piperazin-1-yl]-9H-purine (MK169)

To a solution of **6** (0.04 g, 0.08 mmol) in 2 mL absolute EtOH, PPTS (0.06 g, 0.25 mmol) was added, and the mixture was stirred at room temperature for 18 h. The solvent was then evaporated and the residue was purified by flash column chromatography (CH₂Cl₂/CH₃OH, 97:3 to 9:1 v/v) to afford **MK169** as a white sticky solid (0.02 g, 55% yield); *R_f* = 0.42 (CH₂Cl₂/CH₃OH 9:1 v/v); ¹H NMR (600 MHz, CDCl₃): δ 11.32 (bs, 1H, NH), 8.39 (s, 1H, H-2), 7.92 (s, 1H, H-8), 4.38–4.34 (m, 4H, CH₂-piperazine), 3.80–3.78 (m, 2H, CH₂-piperazine), 3.64–3.62 (m, 2H, CH₂-piperazine), 3.33 (s, 3H, S₂O₂CH₃), 3.19 (t, *J* = 7.3 Hz, 2H), 2.41 (t, *J* = 7.4 Hz, 2H), 1.86–

1.81 (m, 2H), 1.76–1.70 (m, 2H), 1.54–1.51 (m, 2H, CH₂-alkyl); ¹³C NMR (75 MHz, DMSO-*d*₆): δ 170.8, 153.1, 151.8, 151.5, 138.4, 118.9, 50.2, 44.9, 41.0, 35.5, 32.1, 28.7, 27.7, 24.1; ESI-HRMS (*m/z*): calcd. for C₁₆H₂₅N₆O₃S₂ [M+H]⁺ 413.1424; found: 413.1423.

4.1.7 | 4-(2-(4-(9-(Tetrahydropyran-2-yl)-9H-purin-6-yl)piperazin-1-yl)ethoxy) benzothioamide (8)

Piperazinyl purine **A** (0.05 g, 0.17 mmol) and bromide **7** (0.04 g, 0.17 mmol) were dissolved with TEA (0.02 mL) in anhydrous CH₂Cl₂ (3 mL). The resulting mixture was stirred at room temperature for 24 h. H₂O was added, and the aqueous layer was extracted with CH₂Cl₂. The combined organic layers were dried over Na₂SO₄, filtered, and concentrated under reduced pressure. Compound **8** was isolated after flash column chromatography (CH₂Cl₂/CH₃OH 97:3 v/v) as a yellow solid (0.04 g, 48% yield); *R_f* = 0.28 (CH₂Cl₂/CH₃OH 95:5 v/v) ¹H NMR (300 MHz, CDCl₃): δ 8.35 (s, 1H), 7.95 (s, 1H), 7.89 (d, *J* = 8.9 Hz, 2H, ArH), 7.59 (bs, 1H), 7.20 (bs, 1H), 6.90 (d, *J* = 8.9 Hz, 2H, ArH), 5.72 (dd, *J* = 10.2 and 2.4 Hz, 1H, CH-THP), 4.36 (bs, 4H, CH₂ piperazine), 4.21 (t, *J* = 5.6 Hz, 2H), 2.74 (m, 4H, CH₂ piperazine), 2.10–1.61 (m, 6H, CH₂-THP); ¹³C NMR (75 MHz, CDCl₃): δ 201.4, 162.1, 153.8, 152.5, 150.3, 136.2, 131.6, 129.2, 119.9, 114.2, 81.7, 68.9, 66.2, 57.2, 53.8, 50.8, 32.0, 25.0, 23.0; ESI-HRMS (*m/z*): calcd. for C₂₃H₃₀N₇O₂S [M+H]⁺ 468.2176; found: 468.2183.

4.1.8 | 4-(2-(4-(9H-Purin-6-yl)piperazin-1-yl)ethoxy)benzothioamide (MK178)

Purine **8** (0.03 g, 0.06 mmol) was dissolved in 3 mL anhydrous CH₂Cl₂. TFA (0.25 mL, 3.2 mmol) was added, and the solution was stirred at ambient temperature for 30 min. The mixture was then neutralized with saturated aqueous NaHCO₃ solution, and the aqueous phase was extracted with CH₂Cl₂. The combined organic layers were washed with saturated aqueous NaCl solution, dried over Na₂SO₄, filtered, and concentrated in vacuo. The crude material was purified by flash column chromatography (CH₂Cl₂/CH₃OH, 98:2 to 92:8 v/v) to afford the final product **MK178** (0.015 g, 65% yield) as a yellowish sticky solid; *R_f* = 0.04 (CH₂Cl₂/CH₃OH 95:5 v/v); ¹H NMR (300 MHz, DMSO-*d*₆): δ 13.01 (s, 1H), 9.61 (s, 1H), 9.30 (s, 1H), 8.19 (s, 1H, H-2), 8.10 (s, 1H, H-8), 7.94 (d, *J* = 8.9 Hz, 2H, ArH), 6.97 (d, *J* = 8.9 Hz, 2H, ArH), 4.21–4.16 (m, 4H, CH₂ piperazine and 2H, CH₂O), 2.75 (t, *J* = 5.6 Hz, 2H), 2.62–2.58 (m, 4H); ¹³C NMR (75 MHz, DMSO-*d*₆): δ 198.6, 161.2, 153.1, 151.8, 151.4, 138.2, 131.3, 129.5, 118.8, 113.6, 65.7, 56.5, 53.1, 44.6; ESI-HRMS (*m/z*): calcd. for C₁₈H₂₂N₇OS [M+H]⁺ 384.1601; found: 384.1600.

4.1.9 | 6-[4-[2-[(4-Ethoxy)-phenyl]-1,2-dithiole-3-thionyl]-piperazin-1-yl]-9-(tetrahydropyran-2-yl)-9H-purine (10)

A solution of **A** (0.06 g, 0.20 mmol), bromide **9** (0.07 g, 0.20 mmol), and TEA (0.01 mL) in anhydrous CH₂Cl₂ (3 mL) was stirred at room temperature for 20 h. H₂O was then added, and the

aqueous layer was extracted with CH_2Cl_2 . The combined organic layers were washed with saturated aqueous NaCl solution, dried (Na_2SO_4), filtered, and concentrated. Purification by flash column chromatography ($\text{CH}_2\text{Cl}_2/\text{CH}_3\text{OH}$, 7:3 v/v) afforded **10** as an orange solid (0.06 g, 55% yield). $R_f = 0.38$ (EtOAc); ^1H NMR (300 MHz, CDCl_3): δ 8.33 (s, 1H, H-2), 7.94 (s, 1H, H-8), 7.58 (d, $J = 8.8$ Hz, 2H, ArH), 7.35 (s, 1H, CH-dithiole-thione), 6.96 (d, $J = 8.8$ Hz, 2H, ArH), 5.72 (dd, $J = 10.2$ and 2.4 Hz, 1H, CH-THP), 3.83 (bs, 4H, CH_2 piperazine), 4.21 (t, $J = 5.5$ Hz, 2H, CH_2O), 4.15–4.11 (m, 1H), 3.79–3.64 (m, 1H), 2.90 (t, $J = 5.5$ Hz, 2H), 2.75–2.72 (m, 4H), 2.08–1.62 (m, 6H); ^{13}C NMR (75 MHz, CDCl_3): δ 215.3, 173.0, 161.9, 153.8, 152.6, 150.4, 136.4, 134.9, 128.8, 124.7, 120.0, 115.7, 81.8, 69.0, 66.0, 57.1, 53.8, 44.7, 32.0, 25.1, 23.0; ESI-HRMS (m/z): calcd. for $\text{C}_{25}\text{H}_{29}\text{N}_6\text{O}_2\text{S}_3$ $[\text{M}+\text{H}]^+$ 541.1509; found: 541.1513.

4.1.10 | 6-[4-[2-[(4-Ethoxy)-phenyl]-1,2-dithiole-3-thionyl]-piperazin-1-yl]-9H-purine (MK179)

In a solution of analogue **10** (0.03 g, 0.06 mmol) in anhydrous CH_2Cl_2 (2 mL), TFA (0.21 mL, 2.77 mmol) was added, and the reaction mixture was stirred at room temperature for 25 min. The mixture was then quenched with saturated aqueous NaHCO_3 solution (pH = 10). After drying with Na_2SO_4 , the suspension was filtered and the filtrate was purified by flash column chromatography ($\text{CH}_2\text{Cl}_2/\text{CH}_3\text{OH}$ 98:2 v/v) to afford **MK179** as an orange sticky solid (0.012 g, 44% yield); $R_f = 0.13$ ($\text{CH}_2\text{Cl}_2/\text{CH}_3\text{OH}$ 95:5 v/v); ^1H NMR (300 MHz, $\text{DMSO}-d_6$): δ 13.03 (s, 1H, NH), 8.20 (s, 1H, H-2), 8.11 (s, 1H, H-8), 7.87 (d, $J = 8.9$ Hz, 2H, ArH), 7.76 (s, 1H, CH-dithiole-thione), 7.11 (d, $J = 8.9$ Hz, 2H, ArH), 4.26–4.22 (m, 4H, CH_2 -piperazine and 2H, CH_2O), 2.79 (t, $J = 5.5$ Hz, 2H), 2.63 (bs, 4H, CH_2 -piperazine); ^{13}C NMR (75 MHz, $\text{DMSO}-d_6$): δ 215.2, 174.3, 162.4, 153.5, 152.2, 151.8, 138.6, 134.6, 129.5, 124.1, 119.2, 116.0, 66.3, 56.8, 53.5; ESI-HRMS (m/z): calcd. for $\text{C}_{20}\text{H}_{21}\text{N}_6\text{OS}_3$ $[\text{M}+\text{H}]^+$ 457.0933; found: 457.0932.

4.2 | Biology

4.2.1 | Cell Culture

HAoSMCs (Thermo Fisher Scientific, Waltham, MA, USA) were cultured in Gibco smooth muscle cell growth medium M231 supplemented with smooth muscle growth supplement and 0.1 U/mL penicillin + 100 ng/mL streptomycin (PEST, Gibco/Thermo Fisher Scientific) at 37°C and 5% CO_2 . Cells between passages 5–10 were used for the experiments, where 2×10^5 cells/well were seeded in six-well plates and cultured for 24 h before the start of the experiment. The cells were treated for 24 h with vehicle control (dimethyl sulfoxide [DMSO]), 30 $\mu\text{g}/\text{mL}$ of all purine compounds, 100 ng/mL of LPS used as the inflammatory stimulus, or the compounds together with LPS. Cell culture medium was collected and stored at -80°C for further analysis. Purine analogues were dissolved in DMSO. The final concentration of DMSO in culture did not exceed 0.5%.

4.2.2 | Enzyme-linked Immunosorbent Assay

Secreted IL-1 β was measured in the cell culture medium after 24-h treatment using an enzyme-linked immunosorbent assay

(ELISA) kit (DuoSET, R&D Systems, UK) according to manufacturer instructions. Determination of the optical density was measured at 450 nm using a microplate reader, and protein concentrations were calculated using a standard curve of known protein concentrations included in the ELISA kit.

4.2.3 | Statistical Analysis

In all the assays, three independent experiments were analyzed in triplicate. The results are expressed as mean values and standard deviation (SD). The results were analyzed using one-way analysis of variance with Sidak's multiple correction, or the T-test. p -Values < 0.05 were considered statistically significant.

Author Contributions

Dimitra T. Pournara: formal analysis, investigation, and writing – review and editing. **Theano Fotopoulou**: formal analysis, investigation, and writing – review and editing. **Geena Paramel**: formal analysis, investigation, and writing – review and editing. **Madelene Lindkvist**: investigation and writing – review and editing. **Magnus Grenegård**: conceptualization, writing – review and editing, supervision, and funding acquisition. **Karin Fransén**: conceptualization, resources, writing – original draft preparation, writing – review and editing, supervision, and funding acquisition. **Maria Koufaki**: conceptualization, resources, writing – original draft preparation, writing – review and editing, supervision, and funding acquisition.

Acknowledgments

This work was supported by grants from The Knowledge Foundation HÖG2017 #20170191; HÖG2019 #20190088; Synergi2021 #20220083-H-0, Faculty of Medicine and Health #2019-06-13, Örebro University, "OPENSREEN-GR: (MIS) 5002691, co-financed by Greece and the European Union. Dimitra T. Pournara was supported by a fellowship of the Alexander S. Onassis Public Benefit Foundation (PI Maria Koufaki).

The publication of this article in OA mode was financially supported by HEAL-Link.

Conflicts of Interest

The authors declare no conflicts of interest.

Data Availability Statement

The data that support the findings of this study are available from the corresponding author upon reasonable request.

References

1. M. Y. Henein, S. Vancheri, G. Longo, and F. Vancheri, "The Role of Inflammation in Cardiovascular Disease," *International Journal of Molecular Sciences* 23 (2022): 12906, <https://doi.org/10.3390/ijms232112906>.
2. G. K. Hansson, "Inflammatory Mechanisms in Atherosclerosis," *Journal of Thrombosis and Haemostasis* 7, no. Suppl 1 (2009): 328–331, <https://doi.org/10.1111/j.1538-7836.2009.03416.x>.
3. P. M. Ridker, B. M. Everett, T. Thuren, et al., "Antiinflammatory Therapy with Canakinumab for Atherosclerotic Disease," *New England Journal of Medicine* 377 (2017): 1119–1131, <https://doi.org/10.1056/NEJMoal707914>.
4. B. Butts, R. A. Gary, S. B. Dunbar, and J. Butler, "The Importance of NLRP3 Inflammasome in Heart Failure," *Journal of Cardiac Failure* 21 (2015): 586–593, <https://doi.org/10.1016/j.cardfail.2015.04.014>.

5. G. Paramel Varghese, L. Folkersen, R. J. Strawbridge, et al., "NLRP3 Inflammasome Expression and Activation in Human Atherosclerosis," *Journal of the American Heart Association* 5 (2016): e003031, <https://doi.org/10.1161/JAHA.115.003031>.
6. Y. Zheng, L. Xu, N. Dong, and F. Li, "NLRP3 Inflammasome: The Rising Star in Cardiovascular Diseases," *Frontiers in Cardiovascular Medicine* 9 (2022): 927061, <https://doi.org/10.3389/fcvm.2022.927061>.
7. E. Hernandez-Cuellar, K. Tsuchiya, H. Hara, et al., "Cutting Edge: Nitric Oxide Inhibits the NLRP3 Inflammasome," *Journal of Immunology* 189 (2012): 5113–5117, <https://doi.org/10.4049/jimmunol.1202479>.
8. K. Mao, S. Chen, M. Chen, et al., "Nitric Oxide Suppresses NLRP3 Inflammasome Activation and Protects Against LPS-induced Septic Shock," *Cell Research* 23 (2013): 201–212, <https://doi.org/10.1038/cr.2013.6>.
9. P. G. Wang, M. Xian, X. Tang, et al., "Nitric Oxide Donors: Chemical Activities and Biological Applications," *Chemical Reviews* 102 (2002): 1091–1134, <https://doi.org/10.1021/cr000040l>.
10. G. V. Paramel, M. Lindkvist, B. A. Idosa, et al., "Novel Purine Analogues Regulate IL-1 β Release via Inhibition of JAK Activity in Human Aortic Smooth Muscle Cells," *European Journal of Pharmacology* 929 (2022): 175128, <https://doi.org/10.1016/j.ejphar.2022.175128>.
11. I. Andreadou, E. K. Iliodromitis, C. Szabo, and A. Papapetropoulos, "Hydrogen Sulfide and PKG in Ischemia–Reperfusion Injury: Sources, Signaling, Accelerators and Brakes," *Basic Research in Cardiology* 110 (2015): 510, <https://doi.org/10.1007/s00395-015-0510-9>.
12. C. Szabó, "Hydrogen Sulphide and Its Therapeutic Potential," *Nature Reviews Drug Discovery* 6 (2007): 917–935, <https://doi.org/10.1038/nrd2425>.
13. V. Calderone, A. Martelli, L. Testai, V. Citi, and M. C. Breschi, "Using Hydrogen Sulfide to Design and Develop Drugs," *Expert Opinion on Drug Discovery* 11 (2016): 163–175, <https://doi.org/10.1517/17460441.2016.1122590>.
14. C. Zhu, Q. Liu, X. Li, et al., "Hydrogen Sulfide: A New Therapeutic Target in Vascular Diseases," *Frontiers in Endocrinology* 13 (2022): 934231, <https://doi.org/10.3389/fendo.2022.934231>.
15. M. Castelblanco, J. Lugin, D. Ehrichiou, et al., "Hydrogen Sulfide Inhibits NLRP3 Inflammasome Activation and Reduces Cytokine Production both in Vitro and in a Mouse Model of Inflammation," *Journal of Biological Chemistry* 293 (2018): 2546–2557, <https://doi.org/10.1074/jbc.M117.806869>.
16. M. Koufaki, T. Fotopoulou, E. K. Iliodromitis, et al., "Discovery of 6-[4-(6-nitroxyhexanoyl)piperazin-1-yl]-9H-purine, as Pharmacological Post-conditioning Agent," *Bioorganic & Medicinal Chemistry* 20 (2012): 5948–5956, <https://doi.org/10.1016/j.bmc.2012.07.037>.
17. D. T. Pournara, A. Durner, E. Kritsi, et al., "Design, Synthesis, and *in vitro* Evaluation of P2X7 Antagonists," *ChemMedChem* 15 (2020): 2530–2543, <https://doi.org/10.1002/cmdc.202000303>.
18. J. Frantzias, J. Logan, P. Mollat, et al., "Hydrogen Sulphide-releasing Diclofenac Derivatives Inhibit Breast Cancer-induced Osteoclastogenesis In Vitro and Prevent Osteolysis Ex Vivo," *British Journal of Pharmacology* 165 (2012): 1914–1925, <https://doi.org/10.1111/j.1476-5381.2011.01704.x>.
19. K. Kashfi and K. R. Olson, "Biology and Therapeutic Potential of Hydrogen Sulfide and Hydrogen Sulfide-releasing Chimeras," *Biochemical Pharmacology* 85 (2013): 689–703, <https://doi.org/10.1016/j.bcp.2012.10.019>.
20. D. Pournara, G. A. Heropoulos, and M. Koufaki, "Convenient Method for the Synthesis of 5-(4-methoxyphenyl)-3H-1,2-dithiole-3-thione (ADT-OME) and 5-(4-hydroxy phenyl)-3H-1,2-dithiol-3-thione (ADT-OH) Using Microwave Irradiation," *Tetrahedron Letters* 58 (2017): 2378–2380, <https://doi.org/10.1016/j.tetlet.2017.05.010>.

Supporting Information

Additional supporting information can be found online in the Supporting Information section.

Supporting File 1: cbdv70783-sup-0001-SuppMatt.pdf